Electronic Supplementary Information

ATP-responsive nanoparticles for improved chemodynamic therapy and dual starvation therapy

Xiao-Fan Xu,[a] Jun-Tao Chen,[a] Qian Song,[a] Zhi-Qing Wang,[a] Jia-Qin Long,[a] Guo-Jiang Mao,[b] Yongfei Li,[c] Liufang Hu,[a] Juan Ouyang,*[a] and Chun-Yan Li*[a]

[a] Key Laboratory of Environmentally Friendly Chemistry and Applications of Ministry of Education, Key Laboratory for Green Organic Synthesis and Application of Hunan Province, Hunan Provincial University Key Laboratory for Environmental and Ecological Health, College of Chemistry, Xiangtan University, Xiangtan, 411105, PR China.

[b] Henan Key Laboratory of Organic Functional Molecule and Drug Innovation, Collaborative Innovation Center of Henan Province for Green Manufacturing of Fine Chemicals, Key Laboratory of Green Chemical Media and Reactions, Ministry of Education, School of Chemistry and Chemical Engineering, Henan Normal University, Xinxiang, 453007, PR China.

[c] College of Chemical Engineering, Xiangtan University, Xiangtan 411105, PR China.

*Corresponding Author.

E-mail: lichunyan@xtu.edu.cn (Chun-Yan Li), oyj2023@xtu.edu.cn (Juan Ouyang).

Table of contents

Experimental Section

Reagents and instruments: Zinc acetate and bathocuproinedisulfonic acid (BCS) was purchased from Aladdin Reagent (Shanghai, China). Imidazole-2-carboxaldehyde (2-ICA), doxorubicin hydrochloride, copper chloride dihydrate, adenosine triphosphate (ATP), glutathione (GSH), tetramethylbenzidine (TMB), sodium diethyldithiocarbamate trihydrate (DDTC), 5,5'-dithiobis-2-nitrobenzoic acid (DTNB) was purchased from Macklin Reagent (Shanghai, China). GSH kit, GSSG kit and Calcein-AM/PI double staining kit were purchased from Beijing Solarbio Science & Technology Co., Ltd. 4',6-diamidino-2-phenylindole (DAPI) and 2',7'-dichlorofluorescein diacetate (DCFH-DA) were provided by Beyotime (Shanghai, China).

The scanning electron microscopy (SEM) imaging and elemental spectroscopy were performed using a Zeiss Sigma 300 (Germany). The transmission electron microscopy (TEM) imaging was performed by a Japanese JEM-2100 transmission electron microscope (Japan). The electron spectroscopic analysis of elements was performed by X-ray photoelectron spectrometer Thermo Scientific K-Alpha (USA). The powder X-ray diffraction pattern (PXRD) was obtained by Bruker D8-Advance X-ray diffractometer (Germany). The FT-IR spectra were recorded by Bruker Fourier transform infrared spectrometer. The zeta potential and hydrodynamic diameter of nanomaterials were measured in a Zetasizer nano ZS90 (UK) analyzer. The thermogravimetric analysis (TGA) were performed by a METTLER TOLEDO Thermal Analysis System (Switzerland). The absorption spectra were carried out on a

Perkin Elmer Lambda 25 UV/vis spectrophotometer (USA). The fluorescence spectra were collected on a Hitachi F-4600 spectrophotometer (Japan). The fluorescence imaging of cells was obtained by an Olympus FV3000 fluorescence microscope (Japan). The fluorescence imaging of mice was collected on an IVIS Lumina XR small animal optical in vivo imaging system (USA).

Synthesis of ZIF-90 nanoparticles: A DMF solution (2 mL) of zinc acetate dihydrate (0.2 M) was poured into a DMF solution (2 mL) of 2-ICA (0.4 M) under vigorous stirring at room temperature. The mixed solution was sonicated for 5 min at room temperature, and 6 mL of DMF was added to the mixture and the sonication was continued for 20 min in order to stabilize the structure of ZIF-90. The resulting ZIF-90 nanoparticles were then purified by centrifugation (10 000 rpm, 5 min) and washed with DMF once and ethanol in turn for several times. ZIF-90 nanoparticles were then collected and dried under vacuum at room temperature for 24 h.

Synthesis of Cu^{2+}-SK@ZIF-90 nanoparticles: A DMF solution (2 mL) dissolved in zinc acetate dihydrate (0.2 M) and copper chloride dihydrate (0.067 M) was poured and mixed into a DMF solution (2 mL) of imidazole-2-carbaldehyde (0.4 M) and shikonin (SK, 4 mg). The mixed solution was sonicated for 5 min at room temperature, and 6 mL of DMF was added to the mixture and the sonication was continued for 20 min in order to stabilize the structure of Cu^{2+}-SK@ZIF-90. Then, the obtained Cu^{2+}-SK@ZIF-90 nanoparticles were purified by centrifugation (10000 rpm, 5 min), and washed with DMF and ethanol successively for several times. The Cu^{2+}-SK@ZIF-90 nanoparticles were then collected and dried under vacuum at room

temperature for 24 h.

Synthesis of Cu^{2+}-SK-GOD@ZIF-90 nanoparticles: Cu^{2+}-SK@ZIF-90 (4 mg/mL) was dispersed into 10 mL of water, and then glucose oxidase (1 mg/mL) was added and stirred overnight. The prepared mixture was isolated and purified by centrifugation (10 000 rpm, 5 min) to obtain Cu^{2+}-SK-GOD@ZIF-90, and the crude product was washed several times with distilled water. The product Cu^{2+}-SK-GOD@ZIF-90 was collected and dried under vacuum at room temperature for 24 h.

ATP-induced release of Cu^{2+}, SK and GOD: In order to study the release of Cu^{2+}, Cu^{2+}@ZIF-90 nanoparticles (4 mg/mL) were reacted with ATP solutions of different concentrations (0, 2, 4, 6, 8, 10 mM) for 1 h. Then, 0.5 mL DDTC (0.5 mM) was added and the absorption spectra of the solution at 450 nm were measured.

In order to study the release of SK, Cu^{2+}-SK@ZIF-90 nanoparticles (4 mg/mL) were reacted with ATP solutions of different concentrations (0, 2, 4, 6, 8, 10 mM) for 1 h, respectively. Then, the fluorescence spectra of the solution excited at 520 nm were measured.

In order to study the release of GOD, Cu^{2+}-SK-GOD@ZIF-90 (4 mg/mL) was reacted with different concentrations of ATP (0, 1, 2, 4, 6, 8, 10 mM) for 1 h. Glucose (2 mg/mL) was added. 30 min later, the amount of H_2O_2 was determined using a H_2O_2 kit, and pH was measured using a pH meter.

All spectroscopic tests were performed in HEPES buffer solution at pH 7.4.

Depletion of GSH by Cu^{2+}: Ellman's method was used to detect the depleting ability of GSH. GSH (10 mM) was reacted with Cu^{2+}-SK-GOD@ZIF-90 solution of

different concentrations (0, 0.5, 1, 2, 4 mg/mL) for 30 min. Then, 0.5 mL DTNB (0.1 mM, DMSO) was added and the absorption spectra of the solution at 412 nm were measured.

The generation of •OH: To study the ability of Cu^{2+}-SK-GOD@ZIF-90 to generate •OH, Cu^{2+}-SK-GOD@ZIF-90 (4 mg/mL) was treated with different concentrations of ATP (0, 1, 2, 4, 6, 8, 10 mM), GSH (10 mM), and H_2O_2 (10 mM) for 1 h, respectively. Then, 0.5 mL of TMB (0.5 mM) was added and incubated for 30 min. And the absorbance at 650 nm was determined.

Cells culture: 293T, HeLa, and HepG2 cell lines were purchased from Wuhan Proceeds Life Technology Co., Ltd. DMEM medium supplementing with 10% (v/v) fetal bovine serum (FBS, Gibco) and 1 % (w/v) penicillin (100 U/mL)/streptomycin (100 μg/mL) was performed to incubate 293T, HeLa, and HepG2 cells at 37 °C under 5 % CO_2 atmosphere.

ATP-induced release of SK and Cu^{2+} in different cells: In order to study the release ability of SK and Cu^{2+} in different cells, 293T, HeLa and HepG2 cells were inoculated on confocal culture dishes (NETS Co.) and cultured for 24 h for adherence. One group of 293T, HeLa, and HepG2 cells were incubated with Cu^{2+}-SK-GOD@ZIF-90 (4 mg/mL) for 24 h. Another group of 293T, HeLa, and HepG2 cells were treated with apyrase (0.5 U/mL) for 2 h and then incubated with Cu^{2+}-SK-GOD@ZIF-90 (4 mg/mL) for 24 h. Then, the cells were washed three times with PBS and stained with 4, 6-diamino-2-phenylindole (DAPI) for 30 min. Fluorescence imaging was measured by a confocal fluorescence microscope. DAPI channel: λ_{ex} =

405 nm; λ_{em} = 420-500 nm. SK channel: λ_{ex} = 560 nm; λ_{em} = 580-680 nm.

Intracellular GSH depletion: In order to study the capacity of GSH consumption in different cells, 293T, HeLa, and HepG2 cells were inoculated on 12-well plates and cultured for 24 h for adherence. The three cells were incubated with PBS, ZIF-90 (4 mg/mL), Cu^{2+}@ZIF-90 (4 mg/mL), Cu^{2+}-SK@ZIF-90 (4 mg/mL) and Cu^{2+}-SK-GOD@ZIF-90 (4 mg/mL) for 24 h, respectively. Then, the intracellular levels of GSH and GSSG were tested using reduced glutathione (GSH) and oxidized glutathione (GSSG) kits.

In order to confirm that the changes of GSH and GSSG contents in cells are caused by Cu^{2+}, 293T, HeLa, and HepG2 cells were inoculated on 12-well plates and cultured for 24 h for adherence. The cells were divided into two groups. One group was incubated with Cu^{2+}-SK-GOD@ZIF-90 (4 mg/mL) for 24 h. The other group was treated with BCS (200 μM) for 10 h and then incubated with Cu^{2+}-SK-GOD@ZIF-90 (4 mg/mL) for 24 h. Then, the intracellular levels of GSH and GSSG were tested using reduced glutathione (GSH) and oxidized glutathione (GSSG) kits.

Intracellular ROS generation: In order to study the capacity of ROS production of Cu^{2+}-SK-GOD@ZIF-90 in HeLa cells. HeLa cells were inoculated on confocal culture dishes (NETS Co.) and cultured for 24 h for adherence. The cells were incubated with PBS, ZIF-90 (4 mg/mL), Cu^{2+}@ZIF-90 (4 mg/mL), Cu^{2+}-SK@ZIF-90 (4 mg/mL) and Cu^{2+}-SK-GOD@ZIF-90 (4 mg/mL) for 24 h, respectively. Then, DCFH-DA (10 μM) were added and incubated in darkness for 30 min. Fluorescence imaging was measured by a confocal fluorescence microscope. DCFH-

DA channel: λ_{ex} = 488 nm; λ_{em} = 495-555 nm.

Effectiveness of intracellular synergistic therapy: In order to study the synergistic therapeutic effect of Cu^{2+}-SK-GOD@ZIF-90 in cells, 293T and HepG2 cells were inoculated on 24-well plates and cultured for 24 h for adherence. The cells were incubated with different concentrations (0~4 mg/mL) of ZIF-90, Cu^{2+}@ZIF-90, Cu^{2+}-SK@ZIF-90, Cu^{2+}-GOD@ZIF-90 and Cu^{2+}-SK-GOD@ZIF-90 for 24 h, respectively. Then, cell viability was measured by CCK-8 method.

HepG2 cells were inoculated on confocal culture dishes (NETS Co.) and cultured for 24 h for adherence. The cells were incubated with PBS, ZIF-90 (4 mg/mL), Cu^{2+}@ZIF-90 (4 mg/mL), Cu^{2+}-SK@ZIF-90 (4 mg/mL), Cu^{2+}-GOD@ZIF-90 (4 mg/mL) and Cu^{2+}-SK-GOD@ZIF-90 (4 mg/mL) for 24 h. Then, they were stained with Calcein - AM and PI for 20 min. Fluorescence imaging was measured by a confocal fluorescence microscope. Calcein-AM channel: λ_{ex} = 488 nm; λ_{em} = 495-555 nm. PI channel: λ_{ex} = 560 nm; λ_{em} = 580-640 nm.

The anti-tumor efficacy in vivo: 1×10^6/mL HepG2 cells were seeded subcutaneously on the back of BALB/C nude mice to construct tumor-bearing mice models. Anti-tumor studies were performed when the tumor volume reached 100 mm^3 (tumor volume = $a\times b^2/2$, a: maximum diameter, b: minimum diameter).

The mice were randomly divided into five groups (10 mice/group). The mice were injected with PBS, ZIF-90 (4 mg/mL), Cu^{2+}@ZIF-90 (4 mg/mL), Cu^{2+}-SK@ZIF-90 (4 mg/mL) and Cu^{2+}-SK-GOD@ZIF-90 (4 mg/mL) through tail vein and treated every two days, respectively. The tumor volume of the mice were recorded

during 14-days treatment. (Tumor growth inhibition rate = $(1-m_{sample}/m_{PBS})\times100\%$, where m_{sample} and m_{PBS} represent the tumor mass of each group and the average tumor mass of the PBS group, respectively). At 14 days, 4 mice in each group were randomly selected for euthanasia, and major organs and tumors were harvested. The mass of each tumor was measured and the image of each tumor was taken.The remaining mice were continuously monitored for a total duration of 60 days

Major organs and tumors of tumor-bearing mice were made into paraffin sections and stained according to hematoxylin and eosin (H&E) staining procedures. H&E staining samples were observed by optical microscope. For terminal deoxynucleotide transferase dUTP incision end labeling (TUNEL) staining assay, paraffin sections were performed according to the instructions of the one-step TUNEL apoptosis assay kit. The stained sections were kept in darkness and observed by fluorescence microscope.

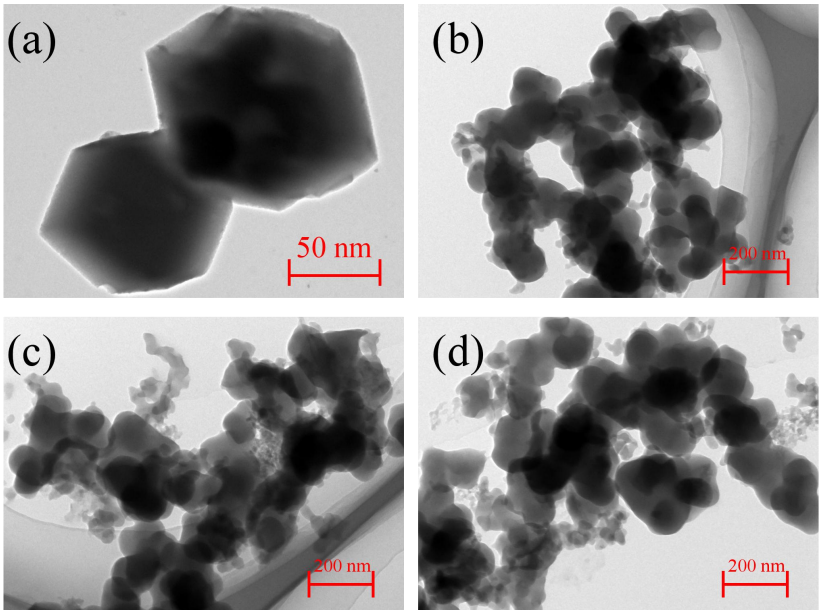

Fig. S1 The TEM images of (a) ZIF-90, (b) Cu^{2+}@ZIF-90, (c) Cu^{2+}-SK@ZIF-90 and (d) Cu^{2+}-SK-GOD@ZIF-90.

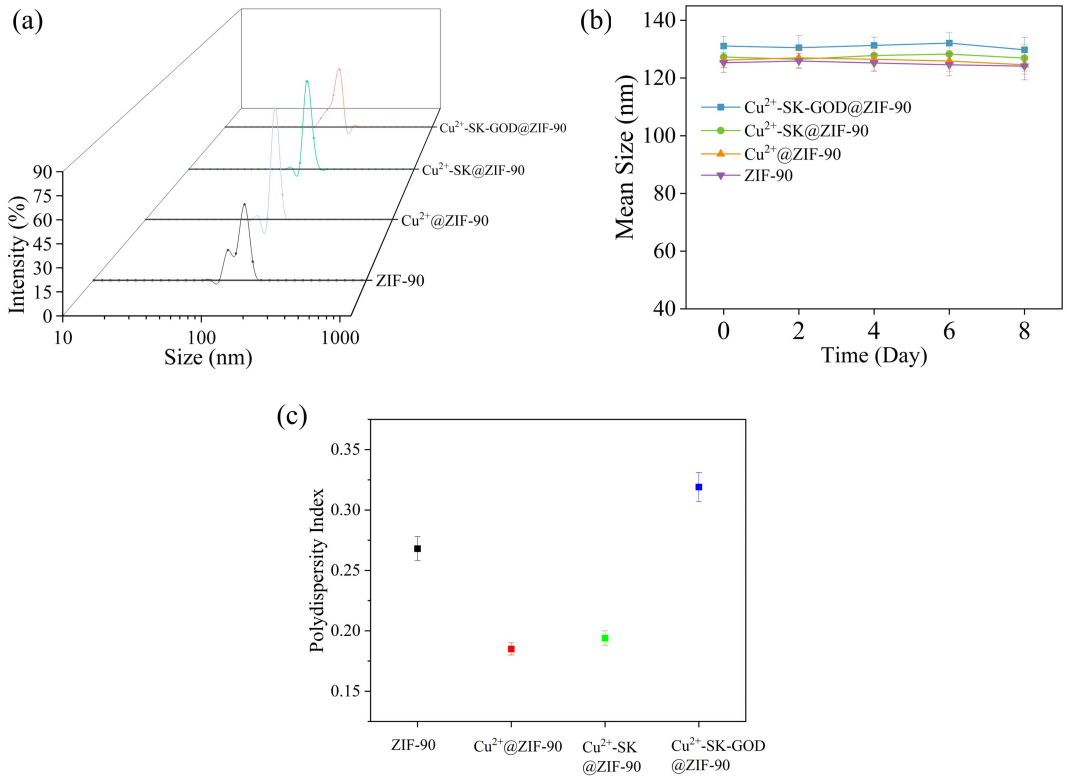

Fig. S2 (a) The dynamic light scattering (DLS) profiles of ZIF-90, Cu^{2+}@ZIF-90, Cu^{2+}-SK@ZIF-90 and Cu^{2+}-SK-GOD@ZIF-90. (b) Hydrodynamic diameters of ZIF-90, Cu^{2+}@ZIF-90, Cu^{2+}-SK@ZIF-90 and Cu^{2+}-SK-GOD@ZIF-90 with times (0, 2, 4, 6, 8 days). (c) Polydispersity index of ZIF-90, Cu^{2+}@ZIF-90, Cu^{2+}-SK@ZIF-90 and Cu^{2+}-SK-GOD@ZIF-90. Data is shown as mean ± S.D. (n = 3).

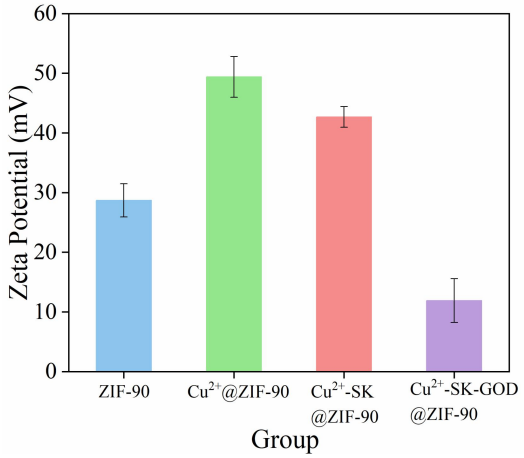

Fig. S3 The Zeta potentials of ZIF-90, Cu^{2+}@ZIF-90, Cu^{2+}-SK@ZIF-90 and Cu^{2+}-SK-GOD@ZIF-90. Data is shown as mean ± S.D. (n = 3).

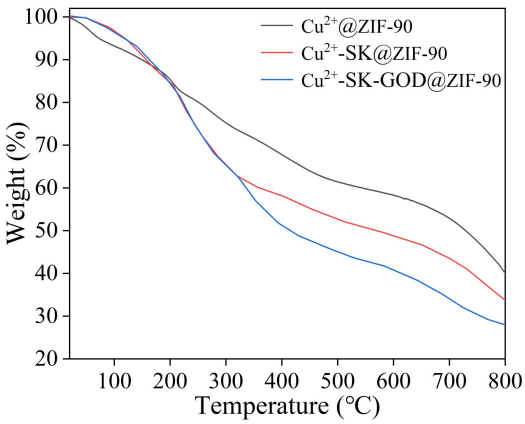

Fig. S4 Thermogravimetric analysis of Cu^{2+}@ZIF-90, Cu^{2+}-SK@ZIF-90 and Cu^{2+}-SK-GOD@ZIF-90.

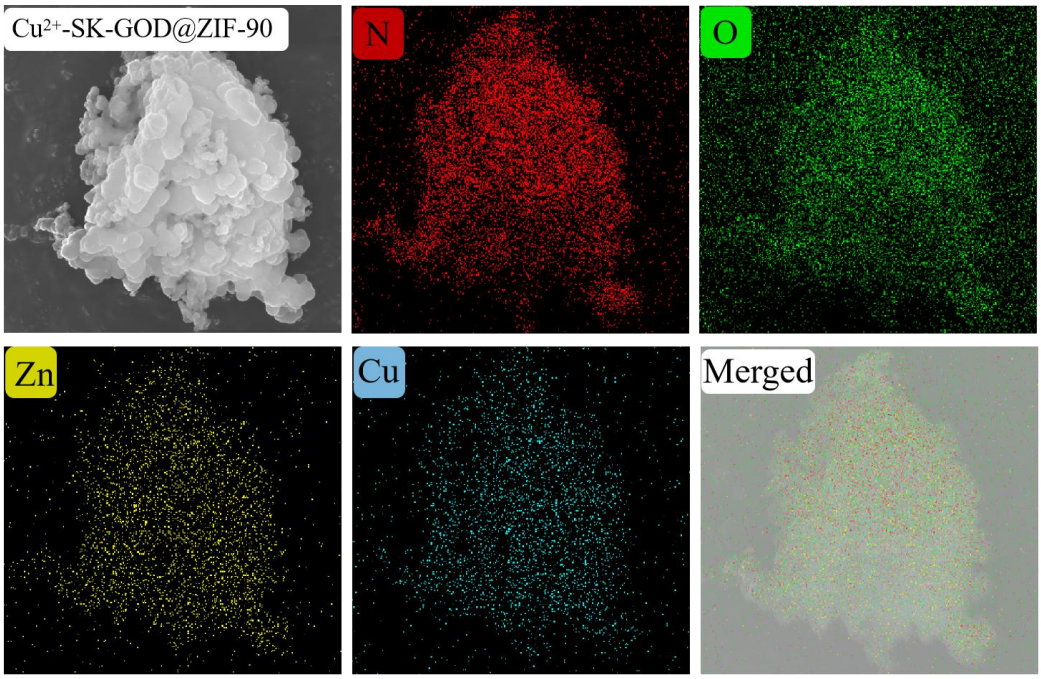

Fig. S5 The corresponding elemental mapping analysis of Cu^{2+}-SK-GOD@ZIF-90.

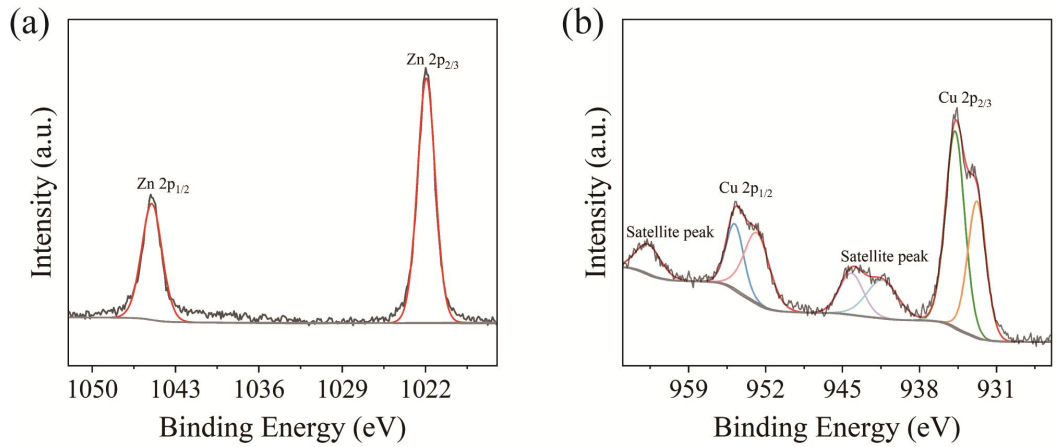

Fig. S6 The high-resolution XPS spectra of (a) Zn 2p region (b) Cu 2p region.

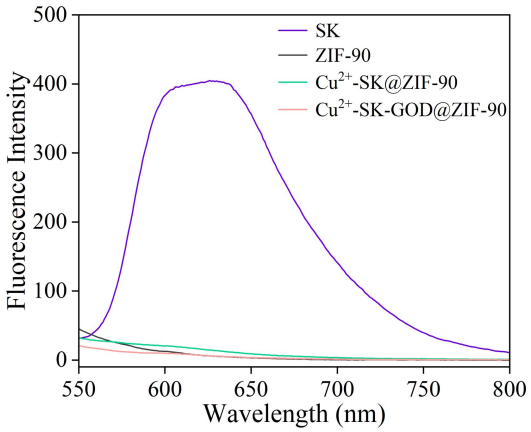

Fig. S7 Fluorescence spectra of SK, ZIF-90, Cu^{2+}-SK@ZIF-90 and Cu^{2+}-SK-GOD@ZIF-90. λ_{ex} = 550 nm.

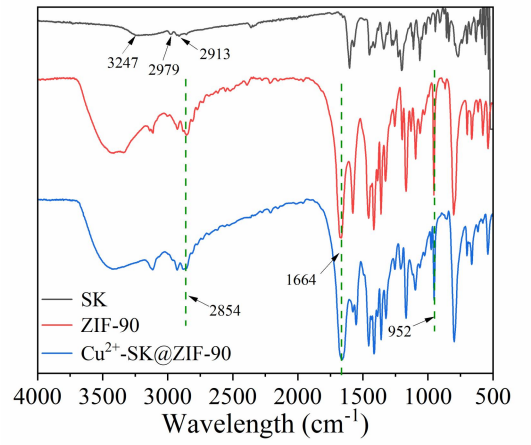

Fig. S8 FT-IR spectra of SK, ZIF-90 and Cu^{2+}-SK@ZIF-90.

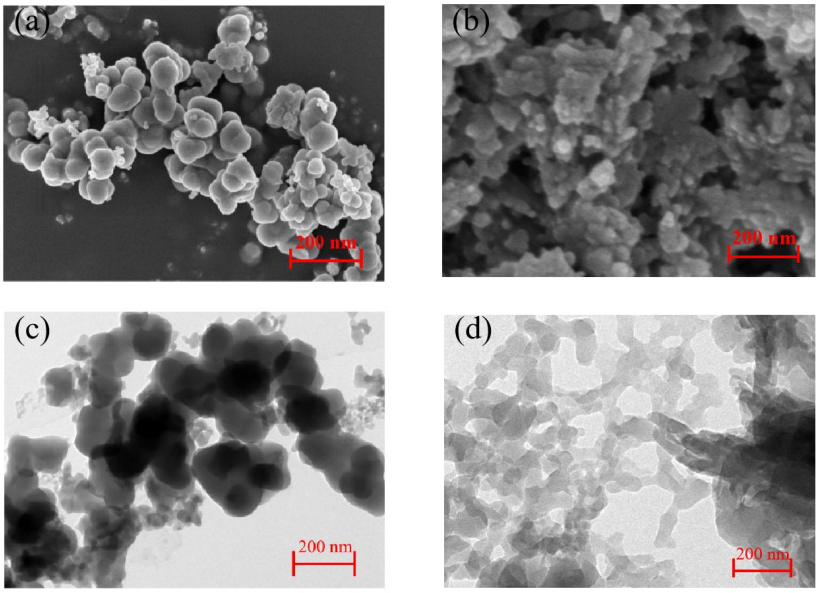

Fig. S9 The SEM images of (a) Cu^{2+}-SK-GOD@ZIF-90 and (b) Cu^{2+}-SK-GOD@ZIF-90 + ATP. The TEM images of (c) Cu^{2+}-SK-GOD@ZIF-90 and (d) Cu^{2+}-SK-GOD@ZIF-90 + ATP.

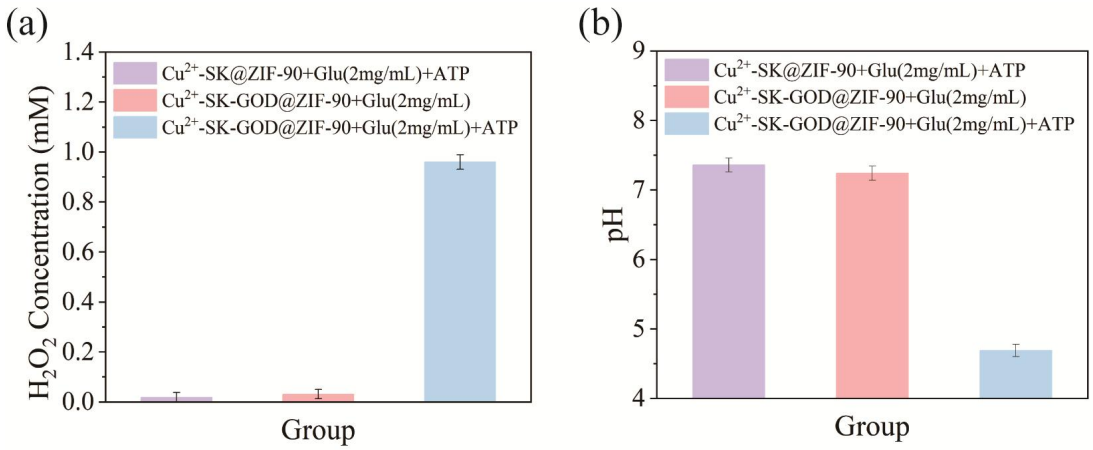

Fig. S10 (a) Concentration of H_2O_2 (b) pH at different conditions for Cu^{2+}-SK@ZIF-90 and Cu^{2+}-SK-GOD@ZIF-90 with ATP (10 mM).

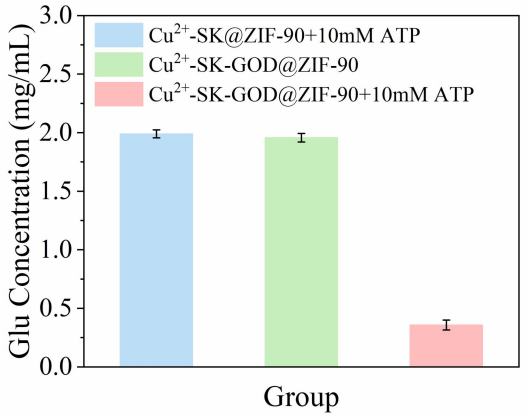

Fig. S11 Concentration of Glu (2 mg/mL) at different conditions for Cu^{2+}-SK@ZIF-90 and Cu^{2+}-SK-GOD@ZIF-90 with ATP (10 mM). The absorbance at 540 nm was measured by the dinitrosalicylic acid method to determine the concentration of Glu.

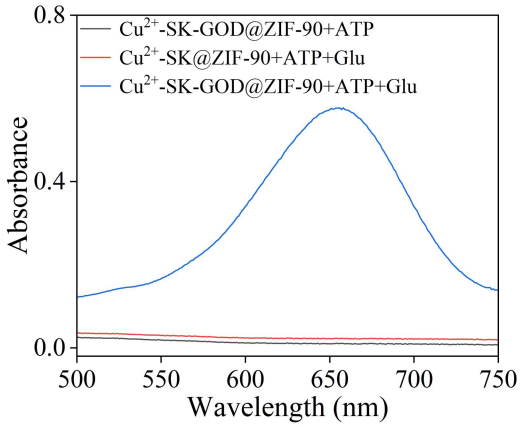

Fig. S12 The production of •OH by Cu^{2+}-SK@ZIF-90 and Cu^{2+}-SK-GOD@ZIF-90 at different conditions (ATP: 10 mM; Glu: 2mg/mL; GSH: 10 mM).

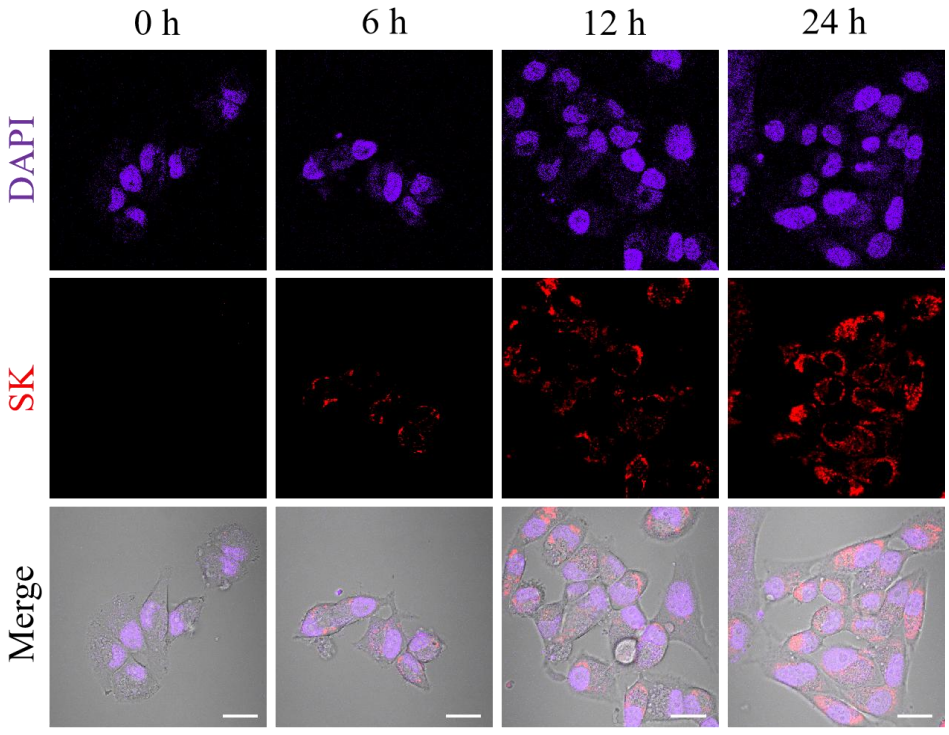

Fig. S13 Fluorescence image of HeLa cells after the incubation with Cu^{2+}-SK-GOD@ZIF-90 (4 mg/mL) for 0, 6, 12, 24 h. DAPI channel: λ_{ex} = 405 nm; λ_{em} = 420-500 nm. SK channel: λ_{ex} = 560nm; λ_{em} = 580-680 nm. Scale bar: 20 μm.

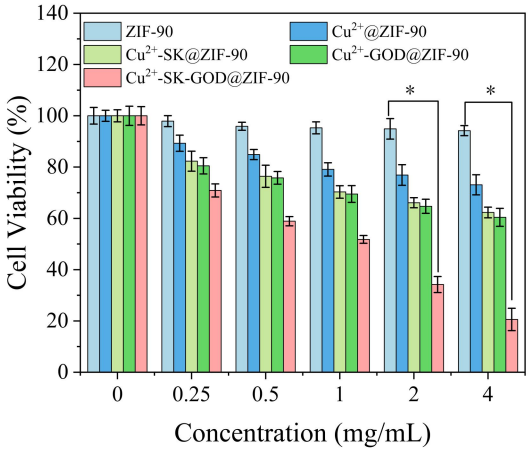

Fig. S14 Cell viability of HeLa cells are treated with different concentrations (0-4 mg/mL) of ZIF-90, Cu^{2+}@ZIF-90, Cu^{2+}-SK@ZIF-90, Cu^{2+}-GOD@ZIF-90 and Cu^{2+}-SK-GOD@ZIF-90.

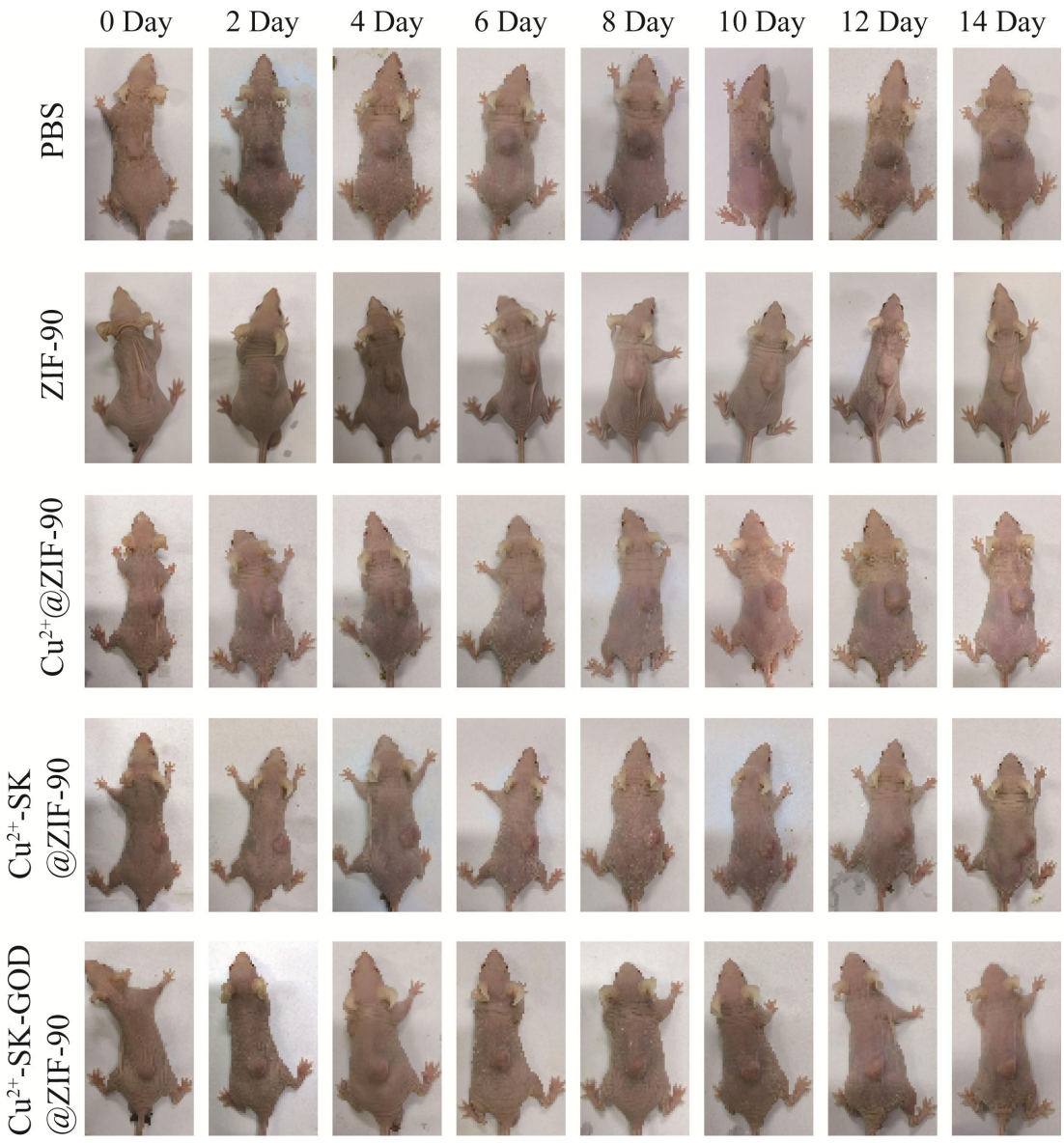

Fig. S15 Photographs of tumor mice treated with PBS, ZIF-90, Cu^{2+}@ZIF-90, Cu^{2+}-SK@ZIF-90 and Cu^{2+}-SK-GOD@ZIF-90.

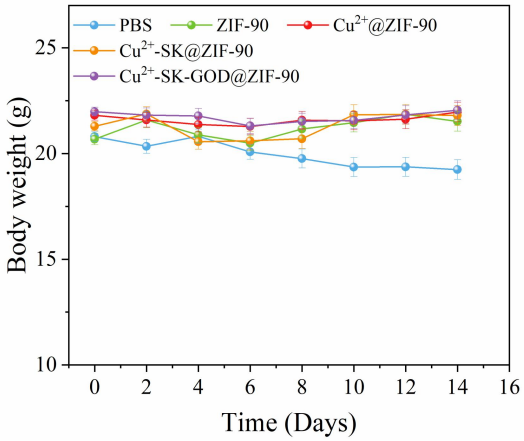

Fig. S16 Body weight of mice treated with PBS, ZIF-90, Cu^{2+}@ZIF-90, Cu^{2+}-SK@ZIF-90 and Cu^{2+}-SK-GOD@ZIF-90.

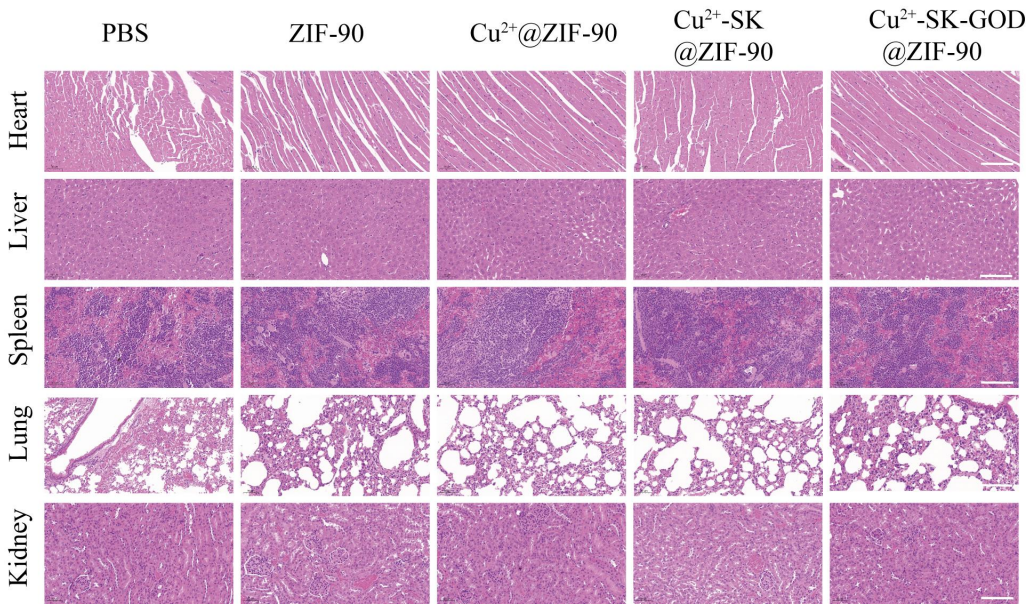

Fig. S17 H&E staining images of major organs (Heart, Liver, Spleen, Lung, Kidney) treated with PBS, ZIF-90, Cu^{2+}@ZIF-90, Cu^{2+}-SK@ZIF-90 and Cu^{2+}-SK-GOD@ZIF-90. Scale bars: 50 μm.